Kinematic and Workspace Analysis of DIAMOND: An Innovative Eye Surgery Robot

Amir Molaei, Ebrahim Abedloo, Hamid D. Taghirad *Senior Member, IEEE* and Zahra Marvi

***Abstract*—this paper presents a new robot for eye surgeries, referred to as DIAMOND. It consists of a spherical mechanism that has a remote center of motion (RCM) point and is capable of orienting the surgical instrument about this unique point. Using the RCM as the insertion point of the surgery instruments makes the robot suitable for minimally invasive surgery applications. DIAMOND has two pairs of identical spherical serial limbs that form a closed kinematic chain leading to high stiffness. The spherical structure of the mechanism is compatible with the human head and the robot may perform the surgery upon the head without any collision with the patient. Furthermore, dexterity and having a compact size is taken into account in the mechanical design of the robot. The workspace of the robot is a complete singularity free sphere that covers the region needed for any eye surgeries. In this paper, a comparison between different types of existing eye surgery robots is presented, the structure of the mechanism is described in detail and kinematic analysis of the robot is investigated.**

I. Introduction

The advent of minimally invasive surgery (MIS) has revolutinized the surgical procedures. MIS provides surgical techniques to perform the surgery through small incisions using a camera and special surgical instruments that are introduced to an internal organ of the body. This method results to less injury, less pain, quicker recovery time and reduced cost of health care. The advantages of MIS method make it an appropriate solution for ocular surgeries such as vitrecomy and glaucoma. In minimally invasive eye surgery the surgeon inserts the surgical tool through a small hole on the sclera and moves it in four degrees of freedom about the incision point. By two rotation the surgical instrument is oriented laterally with respect to the incision point and a translational motion provides the surgeon to access the interior regions inside the eye. Another rotatinal movements about the translational axis can orient the tip of surgical instrument inside the eye. To achieve the minimum injury to the patient through vitroretinal surgery, it is required to hold the incision point fixed which is a tiring task and needs precise movements of the surgical tool. It is also necessary to have a high positioning accuracy about 10 microns which is far more than that of the surgeons hand [1]. The lack of dexterity is another drawback and the vision of the surgical site is not three dimensional. In addition the surgeon cannot touch the interior parts of the eye directly and the sense of the tissue stiffness during surgery is impossible and is beyond the human perception.

The authors are with the Advanced Robotics and Automated Systems (ARAS), Industrial Control Center of Excellence (ICCE), Faculty of Electrical Engineering, K.N. Toosi University of Technology, Tehran, Iran. (Email: Taghirad@kntu.ac.ir)

Advances in robotics technology and computer vision have brought new capabilities that can overcome some limitations of MIS. In robotic surgery, the surgeon uses a master robot to manipulate the instrument attached to slave robot. The computer records the surgeon movements via the master console and controls the slave robot to perform the surgery. Some advantages of robotic surgery are, increased precision motion and removing tremor from hand motion, magnified view of the surgical site, improved dexterity and remote surgery.

Fig. 1. DIAMOND Eye Surgery Robot

For MIS of the eye several robotic arms have been proposed that are some kind of RCMs. The most common type of RCM mechanism are based on parallelogram structures [2],[3],[4]. In this paper we introduce a compact size spherical RCM mechanism referred to as DIAMOND [5]. The robot is illustrated in fig.1. It consist of a spherical parallel mechanism with two degrees of freedom and can move the surgical hand about the RCM point. The surgical hand has two degrees of freedom and translate surgical instrument through the eye and rotates it about the axial axis to orient it's tip. In spherical mechanisms each link may be considered as an arc of a great circle on a sphere. All of the mechanism links are hinged together by revolute joints and the joints axis passes through the center of the sphere which represent the RCM point. Due to orientation of joints axis the mechanism has spherical workspace and all the links have pure rotational movement about the center that induces the RCM of the mechanism. The parallel structure of the mechanism leads to inherent stiffness, while since the actuators are all mounted on the base of the mechanism, it leads to low inertia, and can reach to high velocities and accelerations. Although conventional parallel mechanisms suffer from limited workspace with different

978-1-4799-1972-7/15/$31.00

types of singular points, the workspace of the proposed mechanism is a complete singularity free sphere that covers the region needed for different types of eye surgery. In this paper, the kinematic analysis of the mechanism is given by spherical trigonometry, which makes it much simpler and tractable than cartesian based methods to solve the geometry of spherical structures.

II. Review of Eye Surgery Robots

Da Vinci is the most commonly used and commercially available robot for different MIS surgeries that is approved by FDA of the United States for some surgical procedures [6]. Experiments show that its performance for extraocular surgery is appropriate but it is not efficient for intraocular anterior segment surgery and intraocular posterior segment surgeries [7]. The main reason is that the RCM of mechanism is located 9 cm away of the eye surface. To remedy this problem a Stewart based manipulators is added to the structure to provide a dynamic RCM on the DaVinci's end effector. This provides high dexterity and precision but the range of motion is significantly limited for eye surgeries [7].

For ocular surgeries, some robotic systems have been proposed by researchers. One of the first ocular robotic systems, namely stereotaxical micromanipulator (SMOS), was introduced by Guerrouad and Vidal in 1989 to provide higher precision and dexterity. SMOS has provided operator control using passive input device and has expanded teleoperation to the field of eye surgery for the first time [8],[7],[9]. It of two parts, a career with three degrees of freedom and a wrist with four degrees of freedom [8]. Structure of the wrist is a circular prismatic joint RCM mechanism. As a result, wrist joint variables are spherical coordinate parameters, and the structure is fully isotropic. Despite of the mentioned advantages, the mechanical structure occupy large space around the head of the patient and requires high precision in manufacturing and assembly. Furthermore it cannot be used as a general purpose microsurgery devices [9], [10]. Yu et al in 1998 patented a similar spherical manipulator for drug delivery, physiological measurements using an electrode and etc. These tasks were performed successfully in many operations [7].

A collaboration between NASA-JPL and microdexterity system, Inc (MDS) lead to develop of a telerobotic platform named Robot Assisted Microsurgery (RAMS) invented by Steve Charles at 1997. The robot is light weight and compact with a large workspace greater than 400 cubic centimeters and has six degrees of freedom. Low backlash, 10 microns of precision, high stiffness and back drivability are some of other advantages of RAMS. However, the mechanism has no mechanical RCM that is crucial for most of MIS surgery procedures, especially in vitroretianal surgery, and its control software is complex [7], [11].

The most common RCM structures in different applications are based on parallelogram mechanism. In general, this type of RCM mechanism has a large range of motion, and are very suitable since their actuators can be placed at the base [10]. Madhani et al. [12] introduced a double parallelogram RCM mechanism to overcome the problem of dexterity in MIS surgery at 1998. The black Falcon is an eight DoFs cable driven robot, with four DoFs wrist, one DoF gripper and three DoFs base positioner. This robot can perform common tasks in MIS surgery. One significant feature of black Falcon is back drivability and force reflection [11]. Despite of usual usage of parallelogram based RCM mechanisms they have some inherent problems like intervention between linkages, singularity and lack of absolute rigidity due to a large number of revolute joints[10]. The other eye surgery robot base on parallelogram mechanism is R-HAS robot that is developed in Eindhoven university [13].

One other robot that has been proposed and implemented for minimally invasive surgery is Raven Robot. Raven has seven degrees of freedom manipulator consisting of a static base holding seven actuators and a spherical mechanism that positions surgery tools. The important features of this robot are its haptic feedback, being lightweight and back-drivable [14].

In this paper a parallel spherical RCM mechanism is introduced which is suitable for both general MIS tasks and intraocular surgeries. The closed loop structure of the parallel robot makes it suitably stiff for high accuracy applications. The symmetric design of mechanism leads to tractable dynamic formulation which is favourable in optimization and control schemes. Having a symmetric and simple design the gravity may be compensated very easily by using counter weights. By this means, the mechanism will remain statically stable at any desired configuration that is commanded by surgeon.

One drawback of large surgery robots is the large volume they occupy around the patient and operating table. Such robots are subjected to self-collision, make incorporating force feedback for enhancing the teleoperation task difficult [6]. Having a compact size and the minimum DoF required, makes DIAMOND a very suitable robot that may operate any minimally invasive surgery without such limitations. Due to circular links, it is compatible to human head and can be suitably used in eye surgeries. Having a compact size make it usable in cooperating with other robots simultaneously in a surgery. To represent some features of the robot, motion analysis of the spherical structure of the robot has been investigated. The analysis of spherical mechanisms have been investigated by others [15], [16], [6], [17].The kinematic analysis of DIAMOND is investigated by spherical trigonometry which make the analysis much simpler rather than cartesian based methods.

III. Description of The Robot

A. Robot Structure

Fig. 2 shows the innovated mechanism of DIAMOND Eye Surgery Robot. It is a spherical parallel mechanism whose joints axes intersect at a point which induces the RCM of the mechanism. All the links of the mechanism moves on the surface of a sphere with an arbitrary radius R. The mechanism has two degrees of freedom and can position the eye surgery tool at any desired orientation within the

workspace as it is shown in Fig. 2. The parallel mechanism is composed of two identical serial arms that have common axis at two ends (i. e. , points A and D). The active joints of the mechanism are connected to links 1 and 2 and rotate them about OA that is the common axis of proximal links. The end effector of the robot which holds the surgical tool moves along DO which is the common axis of distal links. The circular length of proximal and distal links are represented by α and β, respectively, and $\vec{a}$, $\vec{b}$, $\vec{c}$ and $\vec{d}$ denote unit vectors along joint axes. The angle of the active joints is measured with respect to ZX plane about Z axis (i. e. θ_1 and θ_2). For any input angles any point of the mechanism moves on a surface of a sphere and its position can be expressed in spherical coordinates. The position of point D is expressed by γ and ϕ in spherical coordinates. The surgical tool is mounted on one of the distal links and has translational motion along $\vec{d}$ or any other radial direction. So, the major problerm in kinematic analysis of the robot is that of the spherical mechanism which is taken account in this paper.

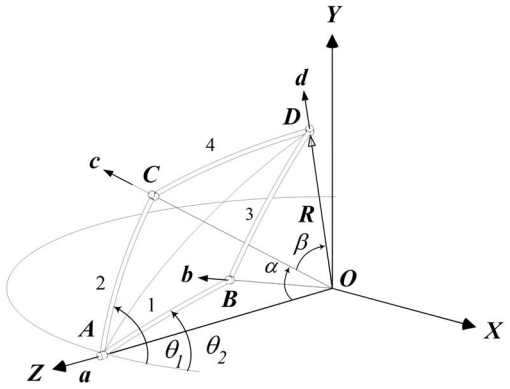

Fig. 2. Schematics of DIAMOND kinematics structure

B. Spherical Trigonometry

A spherical triangle is a graph on a surface of a sphere by three great circular arc intersecting pairwise in three vertices. It is the spherical analog of planar triangle and there are trigonometry identities defined for it, too. For any geometrical configurations, The mechanism forms a spherical polygon that is the spherical analog of planar diamond. The polygon of the mechanism consists of two spherical triangles which can be used to apply spherical trigonometry identities for geometrical analysis of the mechanism. Applying spherical trigonometry for kinematic modeling makes the formulation very simple and there is no need to frame assignment and rotation matrices. Considering a unit sphere for the mechanism, the plane of points **O**, **D**, **A** cuts the sphere on a circular arc that makes two spherical triangles, **ABD** and **ACD**. $\widehat{AD}$ is the common arc of two triangles with an angular length of γ. The position of the point **D** in spherical coordinate is denoted by γ and ϕ. For the spherical triangle **ABD** on a unit sphere, the dihedral angles are measured in radians at the vertices along the surface of the sphere. By dot product of unit vectors the angle of the links are obtained as:

$$\vec{a}\cdot\vec{b}=\cos\alpha,\vec{d}\cdot\vec{b}=\cos\beta \tag{1}$$

Using cross product we can write:

$$\left(\vec{a}\times\vec{b}\right)\cdot\left(\vec{a}\times\vec{d}\right)=\left(|\vec{a}|\left|\vec{b}\right|\sin\alpha\right)\left(|\vec{a}|\left|\vec{d}\right|\sin\gamma\right)\cos A=(\sin\alpha)\left(\sin\gamma\right)\cos A \tag{2}$$

The equation above can be written in the form:

$$\left(\vec{a}\times\vec{b}\right)\cdot\left(\vec{a}\times\vec{d}\right)=\vec{a}\cdot\left[\vec{b}\times\left(\vec{a}\times\vec{d}\right)\right]=\left(\vec{b}\cdot\vec{d}\right)-\left(\vec{a}\cdot\vec{d}\right)\left(\vec{a}\cdot\vec{b}\right)=\cos\beta-\cos\gamma\cdot\cos\alpha \tag{3}$$

Combining last two equations the cosine identity is obtained in spherical geometry with it's two analogous formulas.

$$\begin{aligned}\cos\beta&=\cos\gamma\cdot\cos\alpha+\sin\gamma\cdot\sin\alpha\cdot\cos A\\ \cos\gamma&=\cos\beta\cdot\cos\alpha+\sin\beta\cdot\sin\alpha\cdot\cos B\\ \cos\alpha&=\cos\gamma\cdot\cos\beta+\sin\gamma\cdot\sin\beta\cdot\cos D\end{aligned} \tag{4}$$

Applying the cosine identity for ACD and ABD spherical triangles yields to equality of corresponding dihedral angles that are:

$$\begin{aligned}C\hat{A}D=D\hat{A}B=\hat{A}=(\theta_1-\theta_2)/2\\ B\hat{D}A=C\hat{D}A=\hat{D}\\ A\hat{C}D=A\hat{B}D=\hat{B}=\hat{C}\end{aligned} \tag{5}$$

Using the first equality, dihedral angle of the arc $\widehat{AD}$ with ZX plane is obtained:

$$\varphi=(\theta_1+\theta_2)/2 \tag{6}$$

IV. Kinematic Analysis

A. Forward Kinematics

For kinematic analysis, the RCM serves as the origin of all frames. The angle of the active joints is measured with respect to ZX plane about z axis ($i.e.,\theta_1,\theta_2$). Because the kinematic modeling is independent of R we consider a unit sphere for kinematic analysis and the mechanism links are denoted by spherical angle between two successive joints. The unit vectors **a**, **b**, **c**, **d** are given as follows.

$$\begin{aligned}\vec{a}&=\ [0\quad 0\quad 1]\\ \vec{b}&=\ [\sin\alpha\cdot\cos\theta_2\quad \sin\alpha\cdot\sin\theta_2\quad \cos\alpha]\\ \vec{d}&=\ [\sin\gamma\cdot\cos\varphi\quad \sin\gamma\cdot\sin\varphi\quad \cos\gamma]\\ \vec{c}&=\ [\sin\alpha\cdot\cos\theta_1\quad \sin\alpha\cdot\sin\theta_1\quad \cos\alpha]\end{aligned} \tag{7}$$

Using the unit vectors, ${}^0_iR$ that is the rotation matrix of link i with respect to the base frame can be given as follow:

$${}^0_1R=\begin{bmatrix}\frac{(\vec{a}\times\vec{b})\times\vec{a}}{\sin\alpha} & \frac{\vec{a}\times\vec{b}}{\sin\alpha} & \vec{a}\end{bmatrix}$$

$${}^0_2R=\begin{bmatrix}\frac{(\vec{a}\times\vec{c})\times\vec{a}}{\sin\alpha} & \frac{\vec{a}\times c}{\sin\alpha} & \vec{a}\end{bmatrix}$$

$${}^0_3R=\begin{bmatrix}\frac{(\vec{b}\times\vec{d})\times\vec{b}}{\sin\beta} & \frac{\vec{b}\times\vec{d}}{\sin\beta} & \vec{b}\end{bmatrix} \tag{8}$$

$${}^0_4R=\begin{bmatrix}\frac{(\vec{c}\times\vec{d})\times\vec{c}}{\sin\beta} & \frac{\vec{c}\times\vec{d}}{\sin\beta} & \vec{c}\end{bmatrix}$$

Writing the first cosine identity for **ACD** spherical circle the unknown angles of the mechanism is obtained. The unknown variables for forward kinematics are γ, ϕ and θ_1,θ_2 for inverse kinematics. Using half tangent identities and equation (4) γ is obtained as follow:

$$\gamma_{1,2} = 2\tan^{-1}\left(\frac{s\alpha \cdot c\hat{A} \pm \sqrt{\left(s\alpha \cdot c\hat{A}\right)^2 - \left(c^2\beta - c^2\alpha\right)}}{c\alpha + c\beta}\right) \tag{9}$$

Simplifying the last equation yields:

$$\gamma_{1,2} = 2\tan^{-1}\left(\frac{s\alpha \cdot c\hat{A} \pm \sqrt{s^2\beta - \left(s\alpha \cdot s\hat{A}\right)^2}}{c\alpha + c\beta}\right) \tag{10}$$

The other unknown of the forward kinematics is written as:

$$\varphi = (\theta_1 + \theta_2)/2 \tag{11}$$

B. Inverse Kinematics

For the inverse kinematics unknowns are obtained using the following equations:

$$\begin{aligned} \theta_1 - \theta_2 &= 2\cos^{-1}\left(\frac{\cos\beta - \cos\gamma \cdot \cos\alpha}{\sin\gamma \cdot \sin\alpha}\right) \\ \theta_1 + \theta_2 &= 2\varphi \end{aligned} \tag{12}$$

The last equation is a linear equation of two unknowns and the solution is:

$$\begin{aligned} \theta_1 &= \varphi + \cos^{-1}\left(\frac{\cos\beta - \cos\gamma \cdot \cos\alpha}{\sin\gamma \cdot \sin\alpha}\right) \\ \theta_2 &= \varphi - \cos^{-1}\left(\frac{\cos\beta - \cos\gamma \cdot \cos\alpha}{\sin\gamma \cdot \sin\alpha}\right) \end{aligned} \tag{13}$$

Other dihedral angles of the mechanism are derived as follows using kinematic solution:

$$\begin{aligned} \hat{B} &= \cos^{-1}\left(\frac{\cos\gamma - \cos\beta \cdot \cos\alpha}{\sin\beta \cdot \sin\alpha}\right) \\ \hat{D} &= \cos^{-1}\left(\frac{\cos\alpha - \cos\gamma \cdot \cos\beta}{\sin\gamma \cdot \sin\beta}\right) \end{aligned} \tag{14}$$

C. Multiple Solutions

The inverse kinematic of the mechanism has only one solution and for any geometrical configuration of the mechanism there is one set of input angles. Using equation (9) it is clear that there are two solution for forward kinematics. Considering three different designs, $\alpha = \beta, \alpha < \beta, \alpha > \beta$, their corresponding solution of forward kinematic is shown in fig. 3 . As it is seen in this figure, for non-identical angular link's lengths, one solution is obtained when the proximal links are opened outward and the other is when the links have stretched inwards. Acceptable solution of forward kinematics depends on how the mechanism is assembled. Since, for the special case of equal angular length for distal and proximal links the kinematic equation is simplified as into the following relation:

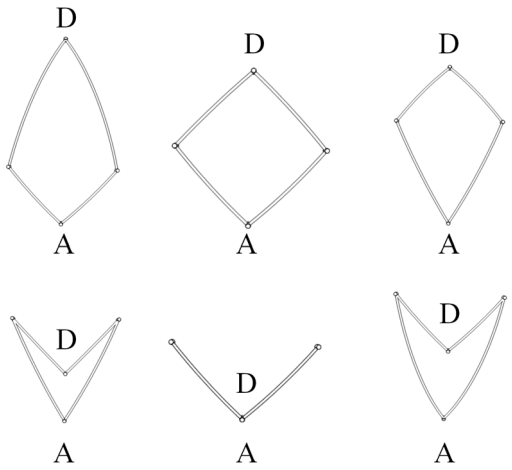

Fig. 3. Schematics of DIAMOND kinematics structure

$$\gamma_{1,2} = 2\tan^{-1}\left(\tan\alpha \cdot \cos\hat{A}\right), 0, \tag{15}$$

Such design is more favorable than the other two cases. Furthermore, as it is shown is section E such design has a larger singularity free workspace.

D. Jacobian Analysis

Jacobian analysis has a major role in kinematic and dynamic analysis of parallel robots. Using the forward kinematic model and differentiating with respect to time the forward Jacobian matrix of the mechanism is obtained as:

$$\dot{\gamma} = -\frac{2s\alpha \cdot s\hat{A}\sqrt{s^2\beta - \left(s\alpha \cdot s\hat{A}\right)^2} \pm (s^2\alpha \cdot s2\hat{A})}{\sqrt{s^2\beta - (s\alpha \cdot sA)^2} \cdot \left(1 + \tan^2\frac{\gamma}{2}\right) \cdot (c\alpha + c\beta)}\dot{\hat{A}} \tag{16}$$

$$\dot{\varphi} = \left(\dot{\theta}_1 + \dot{\theta}_2\right)/2 \tag{17}$$

By denoting the coefficient of $\dot{A}$ in the right hand side of equation (16) as K, one may write:

$$\begin{bmatrix} \dot{\varphi} \\ \dot{\gamma} \end{bmatrix} = \frac{1}{2}\begin{bmatrix} 1 & 1 \\ K & -K \end{bmatrix}\begin{bmatrix} \dot{\theta}_1 \\ \dot{\theta}_2 \end{bmatrix} \tag{18}$$

The angular velocity of proximal links are the same as input angular velocity of actuators and for obtaining the angular velocity of distal links, the time rate of the dihedral angles $\hat{C}$ and $\hat{D}$ is needed. By differentiating equations (14) one may obtain:

$$\begin{aligned} \dot{\hat{B}} &= -\dot{\hat{C}} = \frac{\sin\gamma}{\sin\beta \cdot \sin\alpha \cdot \sin\hat{B}}\dot{\gamma} \\ \dot{\hat{D}} &= \frac{\sin 2\alpha \cdot (1 - 0.5\cos\gamma)}{\left(\sin\gamma\sin\alpha\right)^2 \cdot \sin\hat{D}}\dot{\gamma} \end{aligned} \tag{19}$$

And the angular velocity of proximal and distal links are obtained as:

$$\begin{aligned} w_1 &= \dot{\theta}_1\vec{a} \\ w_2 &= \dot{\theta}_2\vec{a} \\ w_3 &= \dot{\theta}_1\vec{a} - \dot{\hat{B}}\vec{b} \\ w_4 &= \dot{\theta}_2\vec{a} + \dot{\hat{C}}\vec{c} \end{aligned} \tag{20}$$

In which w_i, $(i = 1,2,3,4)$ represents the angular velocity of link i.
For the special case of equal angles of distal and proximal links the Jacobian matrix may be written in the simple form of:

$$\begin{bmatrix} \dot{\varphi} \\ \dot{\gamma} \end{bmatrix} = \begin{bmatrix} 0.5 & 0.5 \\ \dfrac{-\tan\alpha \cdot s\hat{A}}{1+(\tan\alpha \cdot c\hat{A})^2} & \dfrac{\tan\alpha \cdot s\hat{A}}{1+(\tan\alpha \cdot c\hat{A})^2} \end{bmatrix} \begin{bmatrix} \dot{\theta}_1 \\ \dot{\theta}_2 \end{bmatrix} \tag{21}$$

The inverse of Jacobian matrix of the robot maybe derived much simpler than direct inversion of the above matrix, by direct differentiation of inverse kinematic formulations. This will lead to:

$$\begin{aligned} \dot{\theta}_1 &= \dot{\varphi} - \frac{0.5\sin 2\alpha\,(1-\cos\gamma)}{\sqrt{1-\cot\alpha\left(\dfrac{1-\cos\gamma}{\sin\gamma}\right)^2}}\dot{\gamma} \\ \dot{\theta}_2 &= \dot{\varphi} + \frac{0.5\sin 2\alpha\,(1-\cos\gamma)}{\sqrt{1-\cot\alpha\left(\dfrac{1-\cos\gamma}{\sin\gamma}\right)^2}}\dot{\gamma} \end{aligned} \tag{22}$$

E. Robot Workspace

In order to find the boundaries of the workspace, one may search for the configurations in which the Jacobian matrix of the robot becomes singular. The workspace depends on the angular length of proximal and distal links. For any arbitrary angular links of the mechanism the workspace is a spherical cone as shown in fig. 4. and its volume is obtained using the following relation.

$$\text{Volume} = \frac{4}{3}\pi R^3\left(\cos((\alpha-\beta)) - \cos(\alpha+\beta)\right) \tag{23}$$

For $\alpha = \beta = \pi/4$ the workspace of robot is a complete singularity free sphere that fully covers the region needed for any ocular surgery.

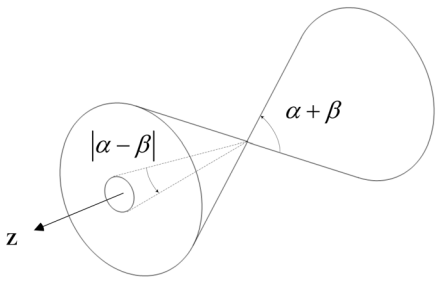

Fig. 4. The Robot General Workspace

V. Verification

To verify kinematic formulations a model of robot has been built in commercial software [1] and for a given trajectory simulation results is compared with that of the model. Verification is done for a model with equal angular length for both proximal and distal links that are $\pi/4$ and the trajectory of joint space is as follow:

$$\theta_1 = -\frac{5}{6}\sin(\pi), \theta_2 = \frac{5}{3}\sin\left(\frac{3}{2}\pi\right) \tag{24}$$

For the given trajectory the workspace variable of the model and simulation is illustrated in fig. 5.

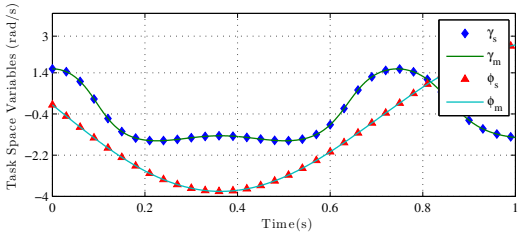

Fig. 5. Task space motion

As it is clearly seen in this figure, the trajectories obtained from simulation and model are completely identical, the accuracy of analysis is of the order of 10^{-7} which is not shown in the graph. The velocity verification results is illustrated in fig. 6 which shows similar trend, with an accuracy of 10^{-6}.

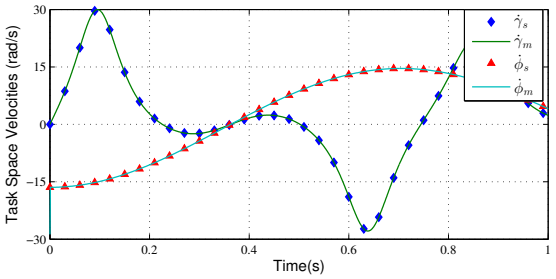

Fig. 6. Task space velocity

VI. Analysis of Kinematic Index

In order to analyze robot dexterity we may investigate some quantitative measures. Several criteria are developed to measure robot dexterity. Yushikava [18] proposed manipulability index that is a local performance measure. It indicates the robot manipulation dexterity inside the workspace and is given by:

$$w = |\det(J)| \tag{25}$$

The manipulability of robot with equal length of links for various $0° < \alpha < 70°$ with 5 degree grid step is illustrated in fig. 7; As it is seen in this figure, this measure get close to zero only at the down end of the curves. Such configurations may be determined by using equation (15). Upon determining such configurations the result indicate that such singularity happens at the maximum value of γ. This singular configurations are at the boundary of the workspace, where both proximal and distal links are completely stretched outward. Therefore, the whole workspace of the robot is singular free.

[1] MSC ADAMS

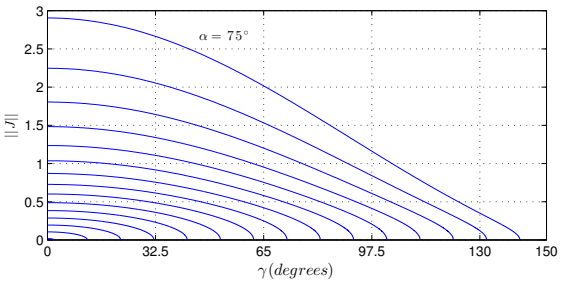

Fig. 7. Manipulability index

The other index for kinematic analysis of the mechanism is condition number which reads as the ratio of largest to smallest singular value of the Jacobian matrix. Fig. 8 illustrates the value of condition number within robot workspace for different value of link angles. As it is shown in this figure, the condition number for all values of α are not very large and lie within a suitable range. Furthermore, for values of α in the region $10^o < \alpha < 45^o$, the condition number lies near one, and such designs are closer to isotropy within a larger volume of workspace. For implementation of the robot the value of α may be set in this region.

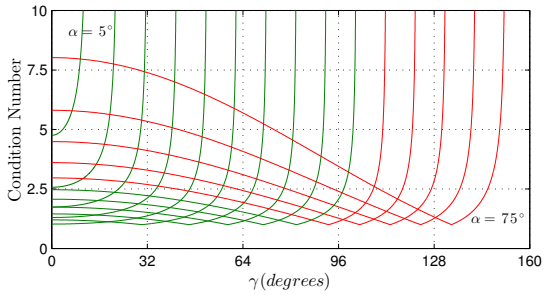

Fig. 8. Condition number

VII. Conclusions

In this paper we introduced a novel spherical parallel RCM mechanism for ocular surgery applications. The parallel structure of mechanism leads to high stiffness and accuracy, while mounting actuators on the base enables it to perform in high velocity maneuvers. Having a symmetric design leads to simple kinematic model and a suitable kinematic performance, as well as, large singularity free workspace. The circular links of the robot make it compatible to operate on human face, and the overall evaluation of this robot shows that it is promising for the new generation of eye surgery robots.

References

[1] Taiga Nakano, Naohiko Sugita, Takashi Ueta, Yasuhiro Tamaki, and Mamoru Mitsuishi. A parallel robot to assist vitreoretinal surgery. *International journal of computer assisted radiology and surgery*, 4(6):517–526, 2009.

[2] N. Simaan, R.H. Taylor, and J.T. Handa. System and method for macro-micro distal dexterity enhancement in micro-surgery of the eye, May 26 2011. US Patent App. 12/992,519.

[3] H.W. Tang, H. van Brussel, J. Peirs, and T. Janssens. Remote centre of motion positioner, May 31 2012. US Patent App. 13/320,582.

[4] P.C.J.N. Rosielle and H.C.M. Meenink. Surgical robot, December 19 2013. US Patent App. 13/971,300.

[5] Amir Molaei Ebrahim Abedloo, Hamid D. Taghirad. Minimally invasive eye surgery, March 2 2014. Iran Patent No. 84812.

[6] Mitchell JH Lum, Jacob Rosen, Mika N Sinanan, and Blake Hannaford. Kinematic optimization of a spherical mechanism for a minimally invasive surgical robot. In *Robotics and Automation, 2004. Proceedings. ICRA'04. 2004 IEEE International Conference on*, volume 1, pages 829–834. IEEE, 2004.

[7] Sajeesh Kumar and Jacques Marescaux. *Telesurgery*. Springer, 2008.

[8] Aicha Guerrouad and Pierre Vidal. Smos: stereotaxical microtelemanipulator for ocular surgery. In *Engineering in Medicine and Biology Society, 1989. Images of the Twenty-First Century., Proceedings of the Annual International Conference of the IEEE Engineering in*, pages 879–880. IEEE, 1989.

[9] Russell H Taylor and Dan Stoianovici. Medical robotics in computer-integrated surgery. *Robotics and Automation, IEEE Transactions on*, 19(5):765–781, 2003.

[10] Pei Xu, Yu Jingjun, and Bi Shusheng Zong Guanghua. Enumeration and type synthesis of one-dof remote-center-of-motion mechanisms. In *The 12th world congress in mechanism an machine science, June*, pages 18–21, 2007.

[11] Steve Charles, Hari Das, Timothy Ohm, Curtis Boswell, Guillermo Rodriguez, Robert Steele, and Dan Istrate. Dexterity-enhanced telerobotic microsurgery. In *Advanced Robotics, 1997. ICAR'97. Proceedings., 8th International Conference on*, pages 5–10. IEEE, 1997.

[12] Akhil J Madhani, Günter Niemeyer, and J Kenneth Salisbury. The black falcon: a teleoperated surgical instrument for minimally invasive surgery. In *Intelligent Robots and Systems, 1998. Proceedings., 1998 IEEE/RSJ International Conference on*, volume 2, pages 936–944. IEEE, 1998.

[13] HCM Meenink and Ir Thijs. *Vitreo-retinal eye surgery robot: sustainable precision*. PhD thesis, PhD thesis, TU Eindhoven, Eindhoven, The Netherlands, ISBN: 978-90-386-2800-4, 2011.

[14] Mitchell JH Lum, Jacob Rosen, Mika N Sinanan, and Blake Hannaford. Optimization of a spherical mechanism for a minimally invasive surgical robot: theoretical and experimental approaches. *Biomedical Engineering, IEEE Transactions on*, 53(7):1440–1445, 2006.

[15] Ebrahim Abedloo, Amir Molaei, and Hamid D Taghirad. Closed-form dynamic formulation of spherical parallel manipulators by gibbs-appell method. In *Robotics and Mechatronics (ICRoM), 2014 Second RSI/ISM International Conference on*, pages 576–581. IEEE, 2014.

[16] R Khezrian, E Abedloo, M Farhadmanesh, and SAA Moosavian. Multi criteria design of a spherical 3-dof parallel manipulator for optimal dynamic performance. In *Robotics and Mechatronics (ICRoM), 2014 Second RSI/ISM International Conference on*, pages 546–551. IEEE, 2014.

[17] Carlos Bombin, Lluis Ros, and Federico Thomas. On the computation of the direct kinematics of parallel spherical mechanisms using bernstein polynomials. In *Robotics and Automation, 2001. Proceedings 2001 ICRA. IEEE International Conference on*, volume 4, pages 3332–3337. IEEE, 2001.

[18] Tsuneo Yoshikawa. Manipulability of robotic mechanisms. *The international journal of Robotics Research*, 4(2):3–9, 1985.